A switched structured-H_∞/IQC closed-loop for adult T1DM patients

D. Henry[1], J. Cieslak[1], D. Gucik-Derigny[1], B. Catargi[2], P.S. Rivadeneira[1,3], A. Ferreira De Loza[4] and H. Ríos[5]

***Abstract*— This paper presents our new results on patient-independent closed–loop for blood glucose regulation, for adult diabetic patients affected by Type-1 Diabetes Mellitus. A switched control solution is proposed to avoid severe hypo- and hyper-glycaemia. The design of the control solution is approached using the structured-H_∞ robust control theory, to account for the inter- and intra-patient variability. Robust stability of the switched control law is proven using the integral quadratic constraint theory. The proposed control solution is assessed using the UVA/Padova T1DM metabolic simulator (v3.2), a benchmark recognized by the US Food and Drug Administration as a substitute for pre-clinical tests.**

I. Introduction

Automated insulin delivery systems have been emerging as a viable technological solution for people with type 1 diabetes mellitus (T1DM), known as artificial pancreas (AP) systems [1]. The objective of such systems is to reduce the duration of hyperglycaemia and avoid hypoglycaemia. APs use numerous algorithms, such as insulin pump control, on-board insulin estimation, hypoglycaemia prevention strategies, etc. This paper is concerned by the control function.

Based on subcutaneous glucose measured by a continuous glucose monitoring (CGM) sensor, a control algorithm commands a pump for continuous subcutaneous insulin infusion. A feedforward completes the insulin delivery, i.e. an additional insulin injection called a "bolus" is also administered when the patient indicates that he/she is about to eat.

Medtronic's Minimed 670G was the first AP to be marketed in 2018, followed by Tandem Diabetes' Tandem Control-IQ, Medtronic's MiniMed 780G, CamDiab's CamAPS FX, Diabeloop's DBLG1 system and finally Omnipod Horizon from Insulet Corporation. For all these systems, the closed loop is based either on a PID (Proportional-Integral-Derivative) control law [2], or on an MPC (Model Predictive Control) law [3]. Other solutions can be found in scientific literature, such as the dynamic inversion technique [4], the learning control strategy [5], the neural inverse optimal control via passivity method [6], the switched LQG approach [7] and the bio-inspired approaches [8], [9].

Another control framework that has attracted attention is the H_∞ framework. In [10], the problem is formulated as an H_∞ reference tracking problem. The glucose tolerance curve of healthy patients is retained as a reference model. In [11], a linear fractional transformation (LFT) structure is constructed for control-oriented analysis purposes. This LFT form is then used with the mixed-sensitivity H_∞ approach [12] and the H_∞ loop shaping technique [9] for control synthesis purposes. The μ synthesis theory is used in [13] to address one of the main inclusion criteria for clinical trials: patient age. However, with a controller of order 46 at the second iteration of the so-called *D-K* iteration algorithm, it is worth to say that the controller is practically useless. Fortunately, the authors proposed a reduced version of order 14, but this is still considered too high for actual implementation in an AP.

Other authors have proposed control solutions within the linear parameter varying (LPV) framework. The polytopic LPV formalism is used with LMI region assignment in [14], to design a switched controller with several switching regions, linked to hypo-, hyper- and euglycaemic situations. In [15], a switched LPV controller with two operating modes (conservative and aggressive) is proposed, combined with a sliding mode safety layer that limits the controller's action based on the on-board insulin estimate. The solution proposed in [16] makes judicious use of the polytopic LPV technique, LMI region assignment and extended Kalman filtering. Note that these solutions are built upon simplified low order models (3 for [14], [15] and 8 for [16]) that do not include several important physiological processes, which are moreover, patient-dependent.

This paper aims at addressing some of the aformentionned drawbacks. Based on our previous work reported in [11], a LFT structure that covers the pharmacokinetics and pharmacodynamics interaction of glucose and insulin in organs and their coupling, is built. The difference with the LFT representation reported in our previous work, is that it considers the effect of the endogenous glucose production. This allows the model to cover the dynamics for glycaemic situations between 50mg/dL and 270mg/dL. Furthermore, the proposed LFT structure carries out inter- and intra-population variability, but, as opposed to [13], the LFT complexity is reduced by introducing the non-structured mutiplicative uncertainty LFT paradigm. Then, in a similar fashion than the LPV solutions aforementioned, two controllers are designed depending on the patient's glycaemia: the first one covers the glycaemia from 120mg/dL up to 270mg/dL, and the second one, the glycaemia between 50mg/dL and 120mg/dL. The structured H_∞ theory is used to design the controllers. This approach is thought particularly adapted since it enables to

[1]:IMS Lab, Univ. Bordeaux, Bordeaux INP, CNRS (UMR 5218), 33405 Talence, France. {david.henry,jerome.cieslak,david.gucik-derigny}@u-bordeaux.fr - [2]:Bordeaux Hospitals, Endocrinology and Metabolic Diseases Unit, Bordeaux, France. bogdan.catargi@chu-bordeaux.fr - [3]: Universidad Nacional de Colombia, Facultad de Minas, Departamento de Energía Eléctrica y Automática, Medellin, Colombia. psrivade@unal.edu.co - [4]:Secihti-UNAM Unidad de Alta Teconología 76230, Querétaro, Mexico. daferreirade@secihti.mx - [5]:Tecnológico Nacional de México/I.T. La Laguna, 27000, Coahuila, México,hriosb@lalaguna.tecnm.mx

fix the controllers' order, overcoming the drawbacks of the μ-synthesis approach proposed by [13], while still managing adequately the uncertainties covered by the LFT (in the H_∞-norm sense). The overall control law then results in switching between the two controllers, depending on the patient's glycaemia. Because such a control law belongs to the class of switching controllers, the integral quadratic constraint (IQC) theory is deployed to establish robust stability guarantee.

A key element of the proposed solution is that the control law is patient-independent. Furthermore, it does not require estimating the carbohydrate content of the meal, but it requires its announcement.

The paper is structured as follows. Section II is dedicated to modelling issues. Section III is concerned by the design of the structured H_∞ controllers and the establishment of robust stability guarantee using the IQC theory. Section IV presents the results from a simulation campaign, and finally Section V gives some concluding remarks.

Notations: $\mathbb{R}$ refers to the real set. $\mathbb{R}^{n\times m}$ denotes the real matrix set of n rows and m columns. For a matrix M, M^* refers to the conjugate transpose of M. I_n denotes the identity matrix of dimension n, and I means the identity matrix of adequate dimension."s" is the Laplace transform variable. For a linear state space model (A, B, C, D), $P(s)$ (or simply P) is its associated Laplace transform. The notation $P : \left[\begin{array}{c|c} A & B \\ \hline C & D \end{array}\right]$ is used in the paper. $P(s)$ is assumed to belong to $\mathbb{R}H_\infty$, defined as the real rational functions set, with $||P||_\infty = \sup_\omega \overline{\sigma}(P(j\omega)) < \infty$, where $\overline{\sigma}(M)$ denotes the maximum singular value of the matrix M. For appropriately dimensioned matrices N and $M = \left(\begin{smallmatrix} M_{11} & M_{12} \\ M_{21} & M_{22} \end{smallmatrix}\right)$, the lower LFT is defined according to $\mathcal{F}_l(M, N) = M_{11} + M_{12}N(I - M_{22}N)^{-1}M_{21}$ and the upper LFT as $\mathcal{F}_u(M, N) = M_{22} + M_{21}N(I - M_{11}N)^{-1}M_{12}$. Consider a LPV system where $x,\ u,\ y$ refer to its state, input and output vectors, respectively. The operator Σ_α is defined such that $y(t) = (\Sigma_\alpha u)(t)$ to describe the equations $\dot{x}(t) = A(\alpha)x + B(\alpha)u(t); y(t) = C(\alpha)x + D(\alpha)u(t)$ for some parameter trajectory $\alpha(t)$. With some abuse, we use the notation $y(s) = \Sigma_\alpha u(s)$. The induced $\mathcal{L}_2$ norm (also called to the gain $\mathcal{L}_2$) is defined by $\sup_{||u||_2 \neq 0} \frac{||y||_2}{||u||_2}$. IQC uses the concept of multipliers. For two multipliers $\Pi_j = \left(\begin{smallmatrix} \Pi_{j1} & \Pi_{j2} \\ \Pi_{j2}^* & \Pi_{j3} \end{smallmatrix}\right), j = 1, 2$, the operator $\mathrm{daug}(.)$ is defined as $\mathrm{daug}(\Pi_1, \Pi_2) = \left(\begin{smallmatrix} \Pi_{11} & 0 & \Pi_{12} & 0 \\ 0 & \Pi_{21} & 0 & \Pi_{22} \\ \Pi_{12}^* & 0 & \Pi_{13} & 0 \\ 0 & \Pi_{22}^* & 0 & \Pi_{23} \end{smallmatrix}\right)$.

II. Modelling issues

In order to avoid duplicating materials of our previous work reported in [11], the following developments are mainly concerned by the derivation of the LFT structures required to design the control solution.

In [17], a family of linear time invariant (LTI) models is constructed from the 19th-order nonlinear model of insulin-glucose dynamics reported in [18]. The key element of the proposed modeling approach is based on finding a family of linear models equivalent to the nonlinear model, based on a sufficiently dense set of points to capture all internal dynamics of the nonlinear model for 11 adult patients with age $\in [22, 56]$y and weight $\in [46, 98]$kg. To be compliant with the standard insulin therapy, glucagon input and related states were removed from the model. Furthermore, three states variables related to endogenous glucose production were removed, namely the state referring to the plasma glucagon, the glucagon action and the delayed static glucagon secretion, since their contribution to the blood glycaemia was considered negligible. The result is a multi-model of order 13 validated for a blood glycaemia evolving between 120mg/dL and 270mg/dL (for the considered patients cohort at least).

However, a deeper analysis of the dynamic for the glycaemia zone [50mg/dL;120mg/dL] reveals that the three states related to the endogenous glucose production finally contribute significantly. Thus, in this work we consider them.

Applying the method reported in [17] for a (dense) set of points n=300, leads to a new set of 16th order models such that

$$\overline{G}_{i,k}(\rho,\varphi) : \left[\begin{array}{c|c} A_{i,k}(\rho,\varphi) & B_{i,k}(\rho,\varphi) \\ \hline C_{i,k}(\rho,\varphi) & 0 \end{array}\right], \quad (1)$$
$$k=1,..,n,\ i=1..,N_p, n \times N_p = 3300$$

The input of $\overline{G}_{i,k}\forall(i,k)$ (denoted i_{ns}, given in pmol/min) is the insulin dose (command of the insulin pump), and the output (denoted G_{sc}, given in mg/dL) is the subcatenous glucose concentration (measured by the CGM sensor). N_p=11 refers to the number of patients. $\rho \in \mathbb{R}^{n_\rho} : |\rho_j| \leq \overline{\rho}_j$, $j=\{1, ..., n_\rho\}$ and $\varphi \in \mathbb{R}^{n_\varphi} : |\varphi_j| \leq \overline{\varphi}_j$, $j=\{1, ..., n_\varphi\}$ are (element-wize bounded) parameter vectors that gather the patient's characteristics such that the weight, the age, etc. Fig. 1 illustrates the mesh map used to determine $\overline{G}_{i,k}\forall(i,k)$ based on nonlinear simulations derived from the model reported in [18]. This family of models is then separated into two sub-families $\overline{G}^{(1)}_{i,k}, k=1,..,n_1, i=1,..,N_p$ and $\overline{G}^{(2)}_{i,k}, k=1,..,n_2, i=1,..,N_p$, so that $\overline{G}^{(1)}_{i,k}$ models the dynamics corresponding to a blood glucose concentration (denoted G_b from now on) in the interval [120mg/dL;270mg/dL] (blue points in Fig.1) and $\overline{G}^{(2)}_{i,k}$ models the dynamics for $G_b \in$ [50mg/dL;120mg/dL] (red points in Fig.1), $\forall(i,k)$.

Two LFTs $\mathcal{F}_u(P^{(1)}, \Delta^{(1)})$ and $\mathcal{F}_u(P^{(2)}, \Delta^{(2)})$ are then derived from $\overline{G}^{(1)}_{i,k}$ and $\overline{G}^{(2)}_{i,k}$ respectively, so that for $j=1,2$ (the variable "s" is omitted for clarity):

$$\mathcal{F}_u(P^{(j)}, \Delta^{(j)}) = \mathcal{F}_u(P^{(j)}_{sc}, \delta^{(j)}_{sc})\mathcal{F}_u(P^{(j)}_b, \delta^{(j)}_b) \quad (2)$$

$$\mathcal{F}_u(P^{(j)}_b, \delta^{(j)}_b) = P_0(s)(1 + W^{(j)}_{\text{unc}}\delta^{(j)}_b) \quad (3)$$

$$W^{(j)}_{\text{unc}} \in \mathbb{R}_+, \delta^{(j)}_b \in \mathbb{R} : |\delta^{(j)}_b| \leq 1, \delta^{(j)}_{sc} \in \mathbb{R} : |\delta^{(j)}_{sc}| \leq 1$$
$$\Delta^{(j)} \in \mathbf{\Delta}^{(j)} = \{diag(\delta^{(j)}_b, \delta^{(j)}_{sc})\}$$

The LFTs $\mathcal{F}_u(P^{(j)}_b, \delta^{(j)}_b)$ capture the (uncertain) parameters $\rho_i, \forall i$, whereas $\mathcal{F}_u(P^{(j)}_{sc}, \delta^{(j)}_{sc})$ capture the (uncertain) elements of φ. The couples $(P_0, W^{(j)}_{\text{unc}})$ are derived to obtain the smallest conservative LFTs, i.e. $W^{(j)}_{\text{unc}}, j=1,2$ are minimal.

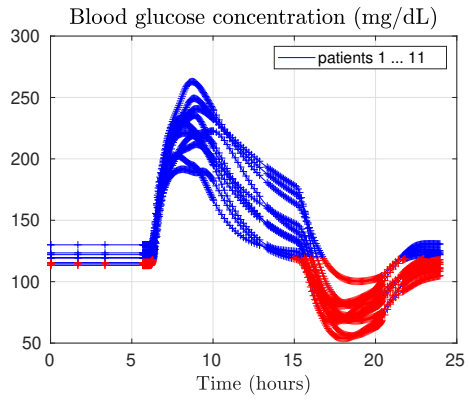

Fig. 1. Mesh map considered for the construction of $G_{i,k}(\rho,\varphi)$

Note that both LFTs $\mathcal{F}_u(P^{(j)},\Delta^{(j)}), j{=}1,2$ share the same nominal model P_0. These two LFTs are nothing else than the model that describes all N_p patients, considering the variability of each of them.

Remark 1: It should be pointed that the CGM sensor and insulin pump are neglected in this modelling process. However, their dynamics and errors are considered for the simulations reported in Section IV. Furthermore, the design of the control algorithm is guided considering them. Especially, the bandwidth of the closed-loop is determined considering the errors and noise of the CGM sensor and constraints to prevent abnormal fatigue of the pump.

III. Design of the Control Algorithm

The control algorithm proposed in this paper is given by (see the notations for the definition of the operator Σ_α)

$$i_{ns}(s){=}\Sigma_\alpha\left(G_{ref}(s)-G_{sc}(s)\right)+i_{anouc}(s) \tag{4}$$

$$\Sigma_\alpha{=}\alpha K^{(1)}(s)+(1-\alpha)K^{(2)}(s) \tag{5}$$

$$\alpha{=}\begin{cases} 0 \text{ if } G_{sc}<120\text{mg/dL} \\ 1 \text{ if } G_{sc}\geq 120\text{mg/dL}\end{cases} \tag{6}$$

where $G_{ref}(t){=}120$mg/dL $\forall t$ is the glucose concentration to track, $i_{anouc}(t)$ is the insulin bolus fixed to 21000pmol/min[1] that is injected at the beginning of the meal, and $G_{sc}(t)$ is the measurement provided by the CGM sensor. Thus, the problem turns out to be:

1) the design of the controllers $K^{(j)}(s), j{=}1,2$.
2) guaranteeing robust stability for arbitrary switching sequence $\alpha(t)$.

The purpose of the following is to address these two issues.

A. Design of $K^{(j)}(s), j{=}1,2$ using structured H_∞ synthesis

In our previous work reported in [11], it is demonstrated that even if the so-called full-order H_∞ and μ-synthesis approaches demonstrate satisfactory performance to control the blood glycaemia, they have the disadvantage to lead to higher order controllers compared to the structured H_∞ approach, which is a well known result in the H_∞/μ control community. Especially, it is demonstrated that a six-order controller guarantees no hypo- and hyperglycaemia. Thus, it is retained six order controllers for $K^{(j)}(s), j{=}1,2$.

Consider the LFTs $\mathcal{F}_u(P^{(j)},\Delta^{(j)}), j{=}1,2$ defined by (2). The problem remains to find $K^{(j)}\in\mathcal{K}^{(j)}$ where

$$\mathcal{K}^{(j)}{=}\left\{K^{(j)}:\begin{array}{r}\dot{x}_K^{(j)}{=}A_K^{(j)}(\kappa)x_K^{(j)}+B_K^{(j)}(\kappa)(G_{ref}-G_{sc}) \\ i_{ns}{=}C_K^{(j)}(\kappa)x_K^{(j)}+D_K^{(j)}(\kappa)(G_{ref}-G_{sc})\end{array}\right\} \tag{7}$$

define the controller spaces, to stabilize the closed loop $\mathcal{F}_l\left(\mathcal{F}_u(P^{(j)},\Delta^{(j)}),K^{(j)}\right)$ internally $\forall\Delta^{(j)}\in\mathbf{\Delta}^{(j)}$: $||\Delta^{(j)}||_\infty\leq 1$, $j{=}1,2$, while achieving some required performance.

It is assumed that the state-space matrices entering in (7) depend smoothly on κ varying in a design space $\mathbb{R}^{n_\kappa}$ or in some constrained subset thereof. Such controllers are denoted as "structured" [19]. As explained, the "structure" retained in this work, corresponds to reduced-order controllers so that the same order is retained for the two controllers $K^{(j)}$, i.e. $\mathcal{K}^{(j)}{=}\mathcal{K}:\dim(x_K^{(j)}){=}6$ for $j{=}1,2$.

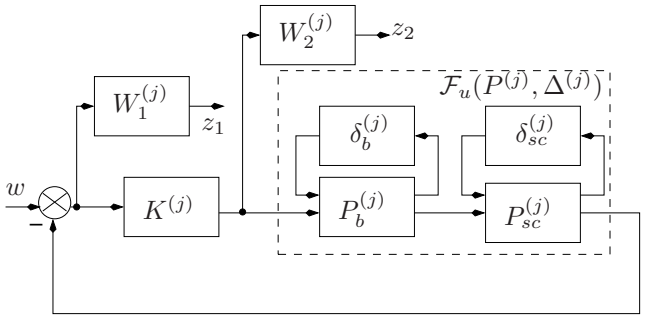

Fig. 2. The mixed sensitivity problem formulation for $K^{(j)}$, $j{=}1,2$.

The problem then turns out to be the design of $K^{(j)}\in\mathcal{K}, j{=}1,2$. This problem is addressed using the mixed sensitivity technique of H_∞ theory, as illustrated in Figure 2. In this approach, the control objectives are guaranteed by an appropriate choice of weighting functions $W_i^{(j)}, j{=}1,2, i{=}1,2$ placed so that the undesirable behaviours of the sensitivity function $S^{(j)}{=}(1+\mathcal{F}_u(P^{(j)},\Delta^{(j)})K^{(j)})^{-1}$ and the control sensitivity function $R^{(j)}{=}K^{(j)}S^{(j)}$, $j{=}1,2$, are penalised in certain fixed frequency ranges *a priori*.

Because it is required to track $G_{ref}(t)$ in low frequencies with the smallest error possible, $W_1^{(j)}$ is chosen as a filtered first-order integrator with cutting frequency $\omega_c^{(j)}$, i.e.:

$$W_1^{(j)}(s){=}k_1^{(j)}\frac{s/\omega_c^{(j)}+1}{s/\omega_l+1},\quad\begin{array}{l}\omega_c^{(1)}{=}4.10^{-3}\text{ rad/min}\\ \omega_c^{(2)}{=}1,5.10^{-3}\text{rad/min}\end{array} \tag{8}$$

$\omega_l{=}10^{-6}$rad/min is an arbitrary low frequency introduced to make $W_1^{(j)}, j{=}1,2$, invertible. $k_1^{(j)}$ is fixed so that the modulus margin is equal to 0.5, at least, i.e. $k_1^{(j)}{=}0.5\frac{\omega_c^{(j)}}{\omega_l}$.

Note that $\omega_c^{(1)}>\omega_c^{(2)}$, so the bandwidth of the closed-loop for the glycaemia ≥ 120mg/dL must be higher than for $G_{sc}<120$mg/dL. In other words, the controller $K^{(1)}$ will be more "aggressive" than $K^{(2)}$.

[1] 3.5 unities in the medical terminology

For $W_2^{(j)}, j$=1, 2, a high–pass filter is chosen to prevent abnormal fatigue of the insulin pump, i.e.

$$W_2^{(j)}(s)=k_2\frac{s/(10\omega_c^{(j)})+1}{s/\pi+1}, k_2=0.1, j=1,2 \quad (9)$$

Then, for a given controller $K^{(j)}$, the problem consists in solving the optimisation problem

$$\begin{aligned}&\text{minimize } \gamma\\ &\text{subject to } \mathcal{F}_l\left(\mathcal{F}_u(P^{(j)},\Delta^{(j)}),K^{(j)}\right) \text{ is internally stable}\\ &K^{(j)}\in\mathcal{K}, \|T_{w\to z_i}\|_\infty\le\gamma,\ i=1,2\end{aligned} \quad (10)$$

where $T_{w\to z_i}$ denotes the transfer between the signals w and z_i i=1, 2, see Fig.2.

This problem can be solved by the tangent-model algorithm proposed in [19]. However and as pointed out by the authors, the resulting algorithm converges to a local minimum in practice.

To overcome this problem, the following practical approach initialy proposed in [11], is adopted: i) The controllers $K^{(j)}, j$=1, 2 are first computed using the μ-synthesis approach; ii) The obtained controllers are next reduced to order 6 using a Grammian-based reduction approach, which iii) are then passed as the initial condition of the tangent-model algorithm presented in [19]. The result is controllers $K^{(j)}, j$=1, 2 practically close to the optimal solution of (10), of order 6, which can easily be embedded in a AP.

To illustrate the results obtained, Fig. 3 shows the sigma plot resulting from the synthesis of $K^{(1)}$ for some fixed values of $\Delta^{(1)}\in\mathbf{\Delta}^{(1)}: ||\Delta^{(1)}||_\infty\le 1$.

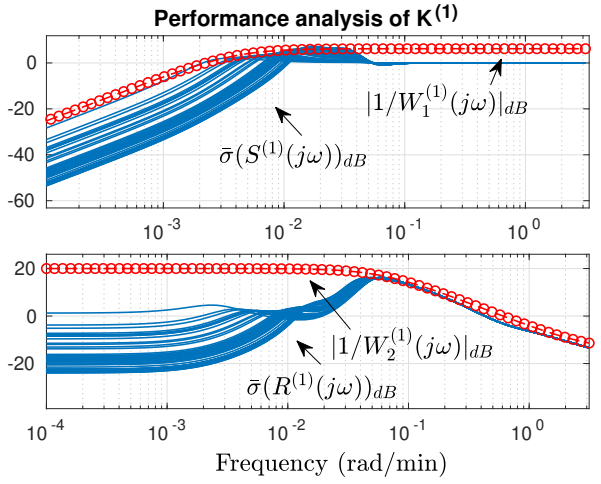

Fig. 3. Sigma plot of $\overline{\sigma}(S^{(1)}(j\omega))$ vs its objective $|W_1^{(1)}(j\omega)|^{-1}$ (top) and $\overline{\sigma}(R^{(1)}(j\omega))$ vs its objective $|W_2^{(1)}(j\omega)|^{-1}$ (bottom).

As it can be seen, $\overline{\sigma}(S^{(1)}(j\omega))<|W_1^{(1)}(j\omega)|^{-1}\ \forall\omega$ and $\overline{\sigma}(R^{(1)}(j\omega))<|W_2^{(1)}(j\omega)|^{-1}\ \forall\omega$, demonstrating that the control objectives specified by the weighting functions $W_1^{(1)}$ and $W_2^{(1)}$ are met, as long as the control law (4)-(6) stays in the mode $\alpha(t)$=1. Similarly, it is obtained $\overline{\sigma}(S^{(2)}(j\omega))<|W_1^{(2)}(j\omega)|^{-1}\ \forall\omega$ and $\overline{\sigma}(R^{(2)}(j\omega))<|W_2^{(2)}(j\omega)|^{-1}\ \forall\omega$ for $K^{(2)}$. However, while these criteria indicate that the synthesis has been successful, there is no stability guarantee for an arbitrary switching sequence $\alpha(t)$. This issue is addressed in the next section using IQC.

B. Robust stability of the switching control law

By including the control law (4)-(6) into a feedback interconnection with the LFTs (2), the LFT $\mathcal{F}_u(\tilde{P},\tilde{\Delta})$ given by

$$\begin{pmatrix}v_\Delta\\G_{sc}\end{pmatrix}=\tilde{P}\begin{pmatrix}w_\Delta\\G_{ref}\end{pmatrix}, w_\Delta=\tilde{\Delta}v_\Delta, \tilde{P}=\begin{pmatrix}\tilde{P}_{\Delta,\Delta}&\tilde{P}_{\Delta,r}\\\tilde{P}_{sc,\Delta}&\tilde{P}_{sc,r}\end{pmatrix} \quad (11)$$

is obtained, where

$$\tilde{\Delta}=diag\left(\delta_b^{(1)},\delta_b^{(2)},\delta_{sc}^{(1)},\delta_{sc}^{(2)},\delta_\alpha(t)\right) \quad (12)$$

with $\delta_\alpha(t)$ accounting for $\alpha(t)$ after normalisation, i.e. $||\delta_\alpha(t)||_{\mathcal{L}_2}\le 1$. This LFT is nothing else than the LFTs $\mathcal{F}_u(P^{(j)},\Delta^{(j)}), j$=1, 2 joined together, closed by the parameter varying controller $K(\alpha)$.

The problem is then to establish internal stability of this closed loop, for all parameter trajectories $\alpha(t)\in[0,1], |\dot{\alpha}|\to\infty$ and $\delta_b^{(j)},\delta_{sc}^{(j)}, j$=1, 2. Such a problem can be addressed using the IQC theory, whose basics can be found in [20], [21].

IQC can be defined in time of frequency domain. Here, the frequency domain is retained with the following definition: Two signals p and q, square integrable on $[0,\infty[$, satisfy the IQC defined by the multiplier Π if and only if

$$\int_{-\infty}^{\infty}\begin{pmatrix}q(j\omega)\\p(j\omega)\end{pmatrix}^*\Pi(j\omega)\begin{pmatrix}q(j\omega)\\p(j\omega)\end{pmatrix}d\omega\ge 0 \quad (13)$$

The following theorem, which a direct application of the results presented in [21] to (11)-(12), solves the robust stability analysis problem of the switching control law (4)-(6)

Theorem 1: For any $\tau\in[0,1]$, let us assume that i) the LFT $\mathcal{F}_u(\tilde{P},\tilde{\Delta})$ is well-posed, ii) $\tau\tilde{\Delta}$ satisfies the IQC defined by Π, and iii) $\forall\omega\in\mathbb{R}_+$, there exists $\epsilon>0$ such that

$$\begin{pmatrix}\tilde{P}_{\Delta,\Delta}(j\omega)\\I\end{pmatrix}^*\Pi(j\omega)\begin{pmatrix}\tilde{P}_{\Delta,\Delta}(j\omega)\\I\end{pmatrix}\le-\epsilon I. \quad (14)$$

where Π is given by $\Pi=\mathrm{daug}(\Pi_1,..,\Pi_5)$ (see the notations for $\mathrm{daug}(.)$), such that for j=1, .., 4,

$$\Pi_j=\begin{pmatrix}\psi_j^*(j\omega)U_j\psi_j(j\omega)&V_j\psi_j(\omega)-\psi_j^*(\omega)V_j^T\\(V_j\psi_j(\omega)-\psi_j^*(\omega)V_j^T)^*&-\psi_j^*(j\omega)U_j\psi_j(j\omega)\end{pmatrix} \quad (15)$$

$$U_j=U_j^T, \psi_j(s)=\begin{pmatrix}1\\F_j(s)\end{pmatrix}, \psi_j^*(j\omega)U_j\psi_j(j\omega)>0 \quad (16)$$

$$\text{and}\quad \Pi_5=\begin{pmatrix}X&Y\\Y^T&-X\end{pmatrix}, X=X^T>0, Y=-Y^T \quad (17)$$

In (16)-(17), $F_j(s), j$=1, .., 4 are first-order low pass filters with a cutting frequency fixed to 1rd/min, U_j, V_j, j=1, .., 4 and X, Y are decision variables in (14). Then, $\mathcal{F}_u(\tilde{P},\tilde{\Delta})$ is stable for all parameter trajectories $\alpha(t)\in[0,1]$ and $\delta_b^{(j)},\delta_{sc}^{(j)}, j$=1, 2. ■

Following Theorem 1, the problem is concerned by solving the infinite-dimension inequality (14). Here, the frequency griding approach proposed in [22] is used. A well-known limitation of a griding method is that it does not guarantee the validity of the solution between two grid points. To overcome this problem, the core idea relies on the fact that in the IQC framework, the $\tilde{\Delta}$ block is not used explicitly. Rather it is replaced by the multiplier Π which "describes" the input/output behaviour of $\tilde{\Delta}$. So the IQC (14) finally depends only on the frequency ω, that is rewritten as a LFT of a real repeated Δ block, by pulling out ω.

Assume a dynamic system $\Sigma : \left[\begin{array}{c|c} \mathcal{A} & \mathcal{B} \\ \hline \mathcal{C} & \mathcal{D} \end{array}\right] : \mathcal{A} \in \mathbb{R}^{m\times m}$ evaluated at a frequency $\omega_0 + \delta\omega \in [\underline{\omega}, \overline{\omega}]$, is written as the lower LFT $\mathcal{F}_l(S(j\omega_0), \delta\omega I_m)$ with

$$S(\omega_0) = \begin{pmatrix} \mathcal{D} & \frac{1}{\sqrt{j}}\mathcal{C} \\ \frac{1}{\sqrt{j}}\mathcal{B} & -j\mathcal{A} \end{pmatrix} \star \left(\frac{1}{\omega_0}\begin{pmatrix} I & I \\ -I & -I \end{pmatrix}\right) \qquad (18)$$

and where "$\star$" corresponds to the interconnection of two LFTs (the so-called star product). If $\overline{\sigma}(\Sigma(j\omega_0)) < 1$, then $\overline{\sigma}(\mathcal{F}_l(S(j\omega_0), \delta\omega I_m)) < 1$ holds true for $\omega_0 + \delta\omega$ and $\underline{\omega} = \omega_0 + \lambda_-^{-1}$, $\overline{\omega} = \omega_0 + \lambda_+^{-1}$, where λ_- and λ_+ are respectively, the real negative and positive eigenvalues of maximal magnitude of the matrix

$$\begin{pmatrix} S_{22} & 0 \\ 0 & S_{22}^* \end{pmatrix} - \begin{pmatrix} 0 & S_{21} \\ S_{12}^* & 0 \end{pmatrix} \begin{pmatrix} I & S_{11} \\ S_{11}^* & I \end{pmatrix}^{-1} \begin{pmatrix} S_{12} & 0 \\ 0 & S_{21}^* \end{pmatrix} \qquad (19)$$

$S_{ij}, (i,j)$=1, 2 are the elements of $S(\omega_0)$ partitioned according to the lower LFT $\mathcal{F}_l(S(j\omega_0), \delta\omega I_m)$, i.e. $\mathcal{F}_l(S(j\omega_0), \delta\omega I_m) = S_{11} + \delta\omega S_{12}(I_m - \delta\omega S_{22})^{-1} S_{21}$.
The iterative algorithm proposed in [22] then consists of:

1) Look for a solution to (14) over a frequency domain griding, which is a LMI feasibility problem in U_j, V_j, X, Y, j=1, .., 4 for a given frequency point.
2) If the LMI problem is not feasible, then there is no solution and the algorithm stops.
3) A frequency domain, where $\overline{\sigma}(\mathcal{F}_l(S(j\omega), \delta\omega I_m)) < 1$ with the solution obtained previously, is computed. If the frequency domain is $[0, +\infty[$, the algorithm stops. Else frequencies where $\overline{\sigma}(\mathcal{F}_l(S(j\omega), \delta\omega I_m)) \geq 1$ are added to the frequency domain griding and the algorithm runs into a new iteration.

Fig. 4 illustrates the result. As it can be seen, the algorithm converges in 3 iterations. The maximum singular value of $\overline{\sigma}(\Sigma(j\omega))$ obtained at each iteration is also presented. Since it can be observed that for the last iteration $\overline{\sigma}(\Sigma(j\omega)) < 1\ \forall\omega$, robust stability of the switching control law (4)-(6) is proved.

IV. Simulations results

The performance of the proposed swithing control law are finally assessed through an intensive simulation campaign, using the UVA/Padova T1DM metabolic simulator (v3.2) [18]. This simulator is recognized by the US Food and Drug Administration as a substitute for pre-clinical testing. The simulator includes a realistic insulin pump model with errors, saturation and quantizer phenomena, as-well-as a standard CGM sensor model as reported in [18].

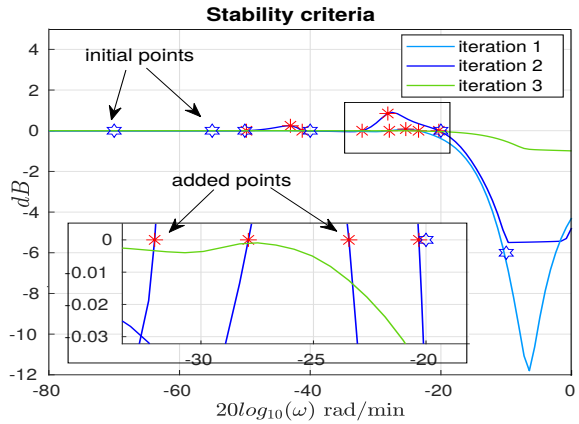

Fig. 4. Robust stability analysis of $\mathcal{F}_u(\tilde{P}, \tilde{\Delta})$.

A total of 11000 runs is performed for a period of 48h. The simulation campaign covers the 11 T1DM adult patients of UVA/Padova. The scenario consists of 3 meals per day: 45 g of carbohydrate at 7:00, 70 g at 13:00 and 60 g at 19:00. All meals have a duration of 20 min. We recall that the characteristics of the patients are: age $\in [22, 56]$y, weight $\in [46, 98]$kg. Fig. 5 illustrates the time-behaviour of the blood glucose concentration $G_b(t)$ and the control signal $i_{ns}(t)$ of the insulin pump, for 110 runs. The switching sequence $\alpha(t)$ is also illustrated. Let us recall that the blood glucose $G_b(t)$ (which is a state) differs from the CGM measurement $G_{sc}(t)$ since there exists a delay due to blood glucose diffusion into interstitial tissues. Nevertheless, the proposed control algorithm exhibits satisfactory performance.

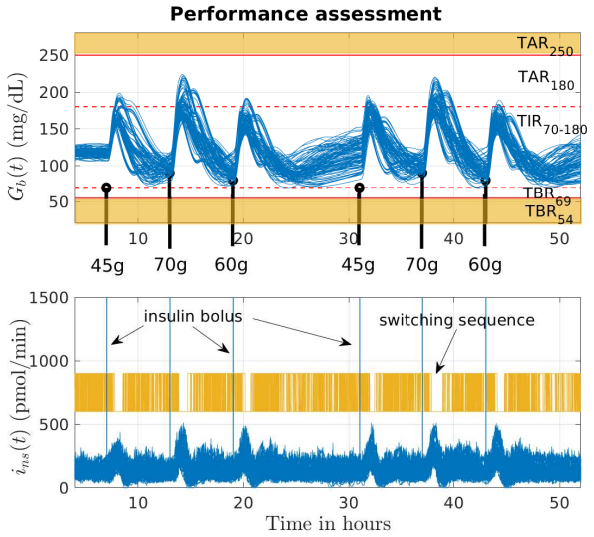

Fig. 5. Simulation campaign for 110 runs covering 11 adult patients: age $\in [22, 56]$y - weight $\in [46, 98]$kg

The simulation results are next analysed by means of clinical metrics, following the metrics advocated in [23]. These clinical specifications are mainly based on blood glucose temporal distribution performance metrics, defined in terms of the "Time above/in/below range specification" metrics,

in percentage, measured on one day. Table I gives the statistics. As it can be seen, no patient demonstrated evidence of hypoglycemia or severe hyperglycemia; glycemic values predominantly remains within the normoglycemic range.

The proposed switching controller is finally compared with the Medtronic PID-based solution [24]. The simulation campaign is conducted in the same conditions than previously described. Table I gives the statistics of the obtained clinical metrics. As it can be seen, the two controls law demonstrate similar performance, but as opposed to the Medtronic's solution that depends on the physiological characteristics of the patients, the solution proposed in this paper does not require any tuning of the controller, which is an advantage.

TABLE I

TIME IN RANGE SPECIFICATION (%)

Criteria		mean	min	max
TAR_{250} (time $>$ 250mg/dL)	$K(\alpha)$	0	0	0
Spec: $< 5\%$	PID	0	0	0
TAR_{180} (time 181-250mg/dL)	$K(\alpha)$	3.29	0	9.74
Spec: $< 25\%$	PID	4	0	15.92
$TIR_{70\text{-}180}$ (time 70-180mg/dL)	$K(\alpha)$	96.73	90.26	100
Spec: $> 70\%$	PID	95.99	84.08	100
TBR_{69} (time 55-69mg/dL)	$K(\alpha)$	0.06	0	0.8
Spec: $< 4\%$	PID	0	0	0
TBR_{54} (time $<$ 54mg/dL)	$K(\alpha)$	0	0	0
Spec: $< 1\%$	PID	0	0	0

V. CONCLUSION

This paper investigated patient-independent closed–loop solutions for blood glucose regulation, for adult diabetic patients affected by Type-1 Diabetes Mellitus. The solution relies on a switching control law, driven by the glycaemia of the patient measured by a CGM sensor. With the help of the linear fractional transformation paradigm, patients variability is modelled and the structured H_∞ robust control theory is used to design the control law. Robust stability of the switched control law is proven using the IQC theory. The proposed solution has been assessed on the 11 T1DM adult patients of the UVA/Padov metabolic simulator (v3.2).The obtained results demonstrated the efficiency of the proposed approach. Finally we argue that the proposed structured controller design/IQC analysis approach offers a promising theory for even more complex metabolic systems.

ACKNOWLEDGMENT

This study has received financial support from the French National Agency (ANR-24-CE51-6734) and the 2025 Visiting Scholar campaign of the University of Bordeaux.

REFERENCES

[1] J.L. Sherr, L. Heinemann, G.A. Fleming, R.M. Bergenstal, D.Bruttomesso, H.Hanaire, R.W. Holl, J.R. Petrie, A.L. Peters, and M.Evans, "Automated Insulin Delivery: Benefits, Challenges, and Recommendations," *Diabetes Care*, vol.45, no.12, pp.3058–3074, 2022.

[2] S. G. M., "Algorithms for a closed-loop artificial pancreas: the case for proportional-integral-derivative control," *Journal of Diabetes Science and Technology*, vol. 7, no. 6, p. 1621–1631, 2013.

[3] B. Bequette, "Algorithms for a closed-loop artificial pancreas: The case for model predictive control," *Journal of Diabetes Science and Technology*, vol. 7, no. 6, p. 1632–1643, 2013.

[4] L. Kovács, P. Szalay, B. Benyó, and G. J. Chase, "Asymptotic output tracking in blood glucose control. a case study," in *2011 50th IEEE Conference on Decision and Control and European Control Conference*, 2011, pp. 59–64.

[5] E. Daskalaki, P. Diem, and S. G. Mougiakakou, "Personalized tuning of a reinforcement learning control algorithm for glucose regulation," in *2013 35th Annual International Conference of the IEEE Engineering in Medicine and Biology Society (EMBC)*, 2013, pp. 3487–3490.

[6] B. S. Leon, A. Y. Alanis, E. N. Sanchez, F. Ornelas-Tellez, and E. Ruiz-Velazquez, "Neural inverse optimal control via passivity for subcutaneous blood glucose regulation in type 1 diabetes mellitus patients," *Intelligent Automation & Soft Computing*, vol. 20, no. 2, pp. 279–295, 2014.

[7] P. Colmegna, F. Garelli, H. De Battista, and R. Sánchez-Pena, "Automatic regulatory control in type 1 diabetes without carbohydrate counting," *Control Engineering Practice*, vol. 74, pp. 22–32, 2018.

[8] I. Pagkalos, P. Herrero, C. Toumazou, and P. Georgiou, "Bio-inspired glucose control in diabetes based on an analogue implementation of a β-cell model," *IEEE Transactions on Biomedical Circuits and Systems*, vol. 8, no. 2, pp. 186–195, 2014.

[9] L. Olçomendy, L. Cassany, A. Pirog, R. Franco, E. Puginier, M. Jaffredo, D. Gucik-Derigny, H. Ríos, and *et al.*, "Towards the integration of an islet-based biosensor in closed-loop therapies for patients with type 1 diabetes," *Frontiers in Endocrinology*, vol. 13, 2022.

[10] E. Ruiz-Velázquez, R. Femat, and D. Campos-Delgado, "Blood glucose control for type I diabetes mellitus: A robust tracking $H\infty$ problem," *Control Engineering Practice*, vol. 12, no. 9, pp. 1179–1195, Sept. 2004.

[11] D. Henry, J. Cieslak, D. Gucik-Derigny, A. F. De Loza, and H. Ríos, "Further results on "non individualized" closed–loop for t1dm patients," in *2023 IEEE Conference on Control Technology and Applications (CCTA)*, 2023, pp. 892–897.

[12] L. Cassany, D. Gucik-Derigny, J. Cieslak, D. Henry, and *et al.*, "A robust H_∞ control approach for blood glucose regulation in Type-1 diabetes," *IFAC-PapersOnLine*, vol. 54, no. 15, pp. 460–465, 2021, 11th IFAC Symposium on Biological and Medical Systems BMS 2021.

[13] E. Ruiz-Velázquez, J. García-Rodríguez, G. Quiroz, and R. Femat, "Robust μ-synthesis: Towards a unified glucose control in adults, adolescents and children with T1DM," *Journal of the Franklin Institute*, vol. 357, no. 14, pp. 9633–9653, 2020.

[14] P. H. Colmegna, R. S. Sánchez-Peña, R. Gondhalekar, E. Dassau, and F. J. Doyle, "Switched lpv glucose control in type 1 diabetes," *IEEE Transactions on Biomedical Engineering*, vol. 63, no. 6, pp. 1192–1200, 2016.

[15] P. H. Colmegna, F. D. Bianchi, and R. S. Sanchez-Pena, "Automatic Glucose Control During Meals and Exercise in Type 1 Diabetes: Proof-of-Concept in Silico Tests Using a Switched LPV Approach," *IEEE Control Systems Letters*, vol. 5, no. 5, pp. 1489–1494, Nov. 2021.

[16] L. Kovács, G. Eigner, M. Siket, and L. Barkai, "Control of diabetes mellitus by advanced robust control solution," *IEEE Access*, vol. 7, pp. 125 609–125 622, 2019.

[17] L. Cassany, D. Gucik-Derigny, J. Cieslak, *et al.*, "A Robust Control solution for Glycaemia Regulation of Type-1 Diabetes Mellitus," in *IEEE European Control Conference*, ser. IEEE European Control Conference. Rotterdam, Netherlands: IEEE, June 2021.

[18] C. Dalla Man, F. Micheletto, D. Lv, *et al.*, "The UVA/PADOVA Type 1 Diabetes Simulator: New Features," *Journal of Diabetes Science and Technology*, vol. 8, no. 1, pp. 26–34, Jan. 2014.

[19] P. Apkarian and N. Doll, "Nonsmooth H_∞ synthesis," *IEEE Transaction on Automatic Control*, vol. 51, no. 1, pp. 71–86, 2006.

[20] J. Veenman, C. W. Scherer, and H. Köroğlu, "Robust stability and performance analysis based on integral quadratic constraints," *European Journal of Control*, vol. 31, pp. 1–32, 2016.

[21] A. Megretski, U. Jönsson, C. Kao, and A. Rantzer, *Integral Quadratic Constraints*, 2nd ed. CRC Press/Balkema, 2018, pp. 1–20.

[22] F. Demourant, "New algorithmic approach based on integral quadratic constraints for stability analysis of high order models," in *2013 European Control Conference (ECC)*, 2013, pp. 359–364.

[23] T. Battelino, T. Danne, R. M. Bergenstal, *et al.*, "Clinical Targets for Continuous Glucose Monitoring Data Interpretation: Recommendations From the International Consensus on Time in Range," *Diabetes Care*, vol. 42, no. 8, pp. 1593–1603, 2019.

[24] Medtronic, "Minimed 670G: a hybrid closed-loop insulin delivery system," *The Medical Letter on Drugs and Therapeutics*, vol. 58, no. 1508, p. 147–148, 2016.